E-Journal of Advanced Maintenance Vol.3-3 (2011) 92-101
Japan Society of Maintenology

Simulation and visualization of guided wave propagation by large-scale 3D FEM

Takashi FURUKAWA* and Ichiro KOMURA
Japan Power Engineering and Inspection Corporation, 14-1 Bentencho, Tsurumi-ku, Yokohama 230-0044, Japan

(Received; For the use of JSM)

Abstract. Ultrasonic guided waves have been widely applied to the long-range inspection of straight piping. The interpretation of the guided wave ultrasonic testing data beyond welds and elbows is challenging because there are many wave modes with different sound velocity. One of the key techniques to examine the beam path of each guided wave mode is the visualization of ultrasonic wave propagation. The authors have employed a large-scale FEM code for bulk wave propagation to the interpretation of UT data, analysis of suitable UT condition and training of UT. This paper describes the simulation and visualization of guided wave propagation in pipes and beyond elbows and welds via a large-scale 3D pure FEM code, which has over one billion elements and parallel computing system. This study presents the comparisons between the simulated and experimental results.

KEYWORDS: Ultrasonic guided wave, Wave propagation, FEM, Piping, Elbow, Welds

1. Introduction

Ultrasonic guided waves are suitable for the long-range inspection and online monitoring of pipes [1-4]. Guided waves in piping are a combination of various wave modes. Each wave mode has a different sound velocity that depends on frequency except for T(0,1) mode. Therefore, guided wave inspection results are difficult to interpret, i.e., a beam path is difficult to extract from observed echoes. Theoretical analyses tools, such as modal analyses, mathematical calculation [5], and semi-analytic numerical calculation [6] help in the planning the inspection setup as well as the interpretation of the inspection results for simple situations. However, the use of a large-scale FEM code is the most effective method for solving the guided wave propagation problem for more complicated situations involving welding, elbows, and defects. The purpose of this research is to confirm the applicability of a large-scale FEM code and a parallel computing technique for the simulation of guided wave propagation and the prediction of echoes in the presence of complex geometries. This paper presents a guided wave transmitting and receiving FEM for guided wave propagation and echo prediction, and compares simulation, theoretical, and experimental results.

2. FEM code and modeling

2.1. FEM code and computing system

A commercial FEM code ComWAVE [7] developed by ITOCHU Techno-Solutions for large-scale 3D analysis was selected to calculate to numerically solve the guided wave propagation problem. A 12-core PC with 96GByte memory and 60-core cluster computing system with 124GByte memory were employed to perform the necessary computations.

*Corresponding author, E-mail: furukawa-takashi@japeic.or.jp

2.2. Guided wave excitation and receiving model

Figure 1 shows the bird views of the FEM mode of pipe (blue area) and probe element(s) (red area). Figure 1(a) shows a single ring-type probe element and Fig. 1(b) shows array-type probe elements. The model was excited by applying the initial displacement vector at all FEM meshed of each probe element(s); examples of the excitation model are shown in Fig. 2. The white arrows indicate the direction of the initial displacement vector. Figure 2(a) shows an excitation model of the torsional mode (T-mode) and Fig. 2(b) and 2(c) show excitation models of the longitudinal mode (L-mode).

The receiving of the model was realized by detecting the 3D displacement waveform at any FEM mesh, corresponding to the receiver position.

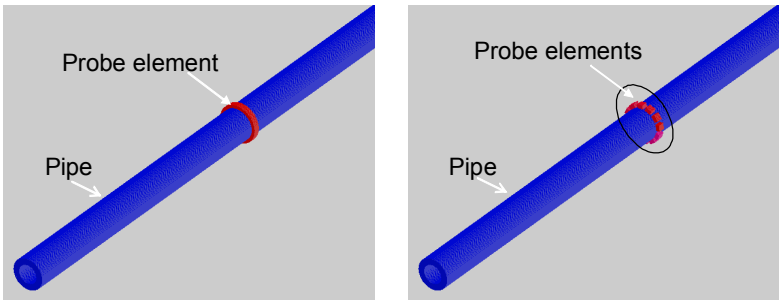

(a) Single ring element **(b) Array-type elements**

Fig. 1. Model of probe element(s) for guided wave excitation

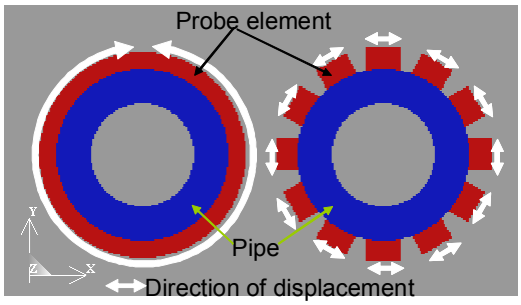

(a) T-mode excitation by single ring or array type element(s) applying circumferential vibration

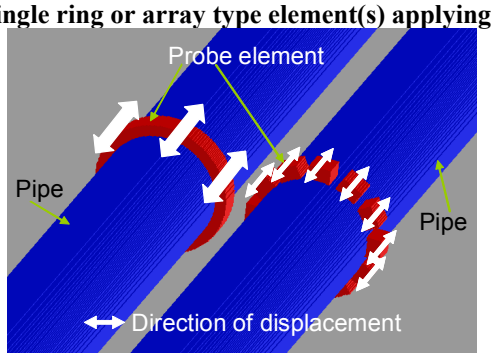

(b) L-mode excitation by single ring or array type element(s) applying axial vibration

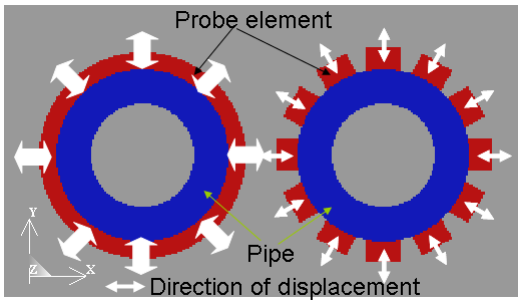

(c) L-mode excitation by single ring or array type element(s) applying radial vibration

Fig. 2. Guided wave excitation model

2.3. FEM model and simulation conditions

The structure of model was divided into cubic elements, with the maximum size of the elements less than one-fifteenth of the wavelength. Figure 3 shows the straight pipe model that was used to verify the modeling by comparing the theoretical and experimental results. Figure 3(a) shows a small two-pipe model of the same dimensions. The dimensions of each pipe are 150 mm in length, 5 mm in outer diameter and 1mm in thickness. The ring-type model, shown in Fig. 2(b), excited the L-mode guided wave. The waveforms of the initial displacements were tone burst signals with five cycles at 200 kHz and 1,000 kHz. Figure 3(b) shows a straight pipe model which dimensions are 2,000 mm in length, 34 mm in outer diameter and 3.2 mm in thickness. Tone burst signals at 200 kHz were emitted from the probe element in the pipe model. The probe element generated the L-mode guided wave as shown in Fig.2(c). The echo signal was detected at outer surface of the pipe near the probe element. The distance between the probe element and receiver was 50 mm. This setup was a model of an experimental setup conducted by Matsuo and Cho [8].

Figure 4 shows the straight pipes and 90° elbow model with two welds. The outer diameter and thickness of model are 60 mm and 4 mm, respectively. Figure 4(a) shows an overview of the model and Fig. 4(b) shows an enlarged view of the elbow and welds. Five cycles of wave, which had center frequency of 30 kHz and 50 kHz, were used for the T-mode excitation of this model, as shown in Fig. 2(a). After traveling about 900 mm beyond the elbow, guided waves are received at eight positions on the outer surface of pipe, as shown in Figs. 4(a) and 4(c).

The material parameters used in the calculation are listed in Table 1.

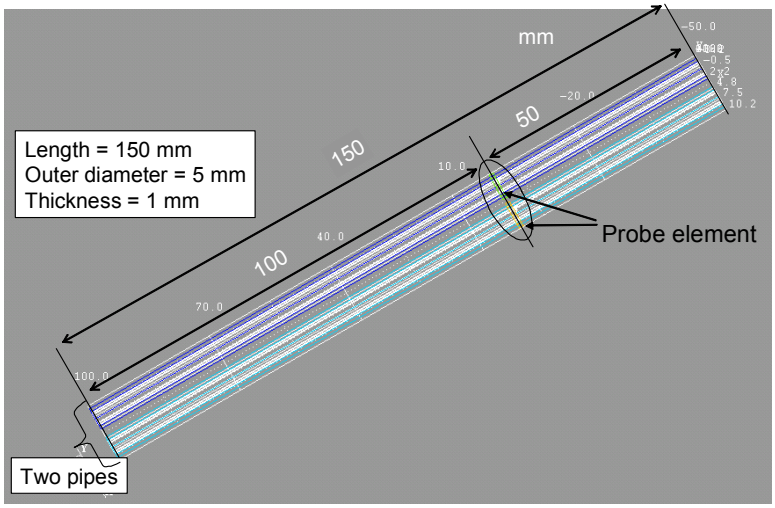

(a) Overview of small two pipes model (Model 1)

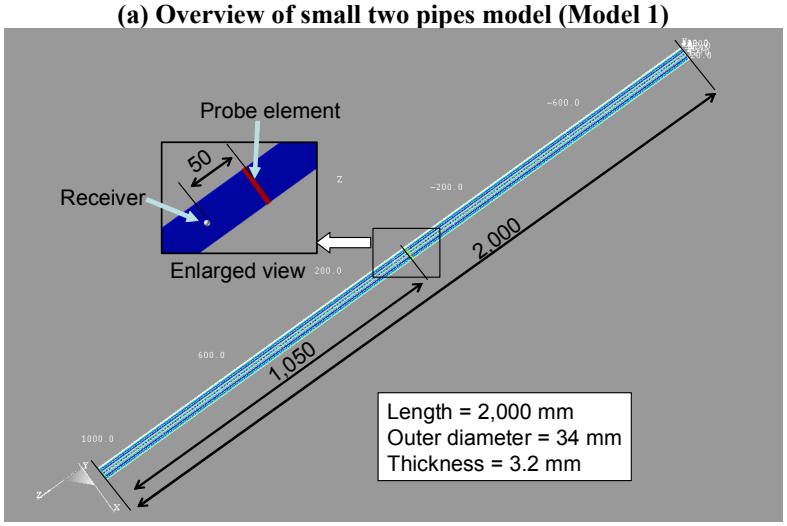

(b) Overview of stainless pipe model (Model 2)

Fig. 3. Straight pipes model for verification (Mode1 1 and 2)

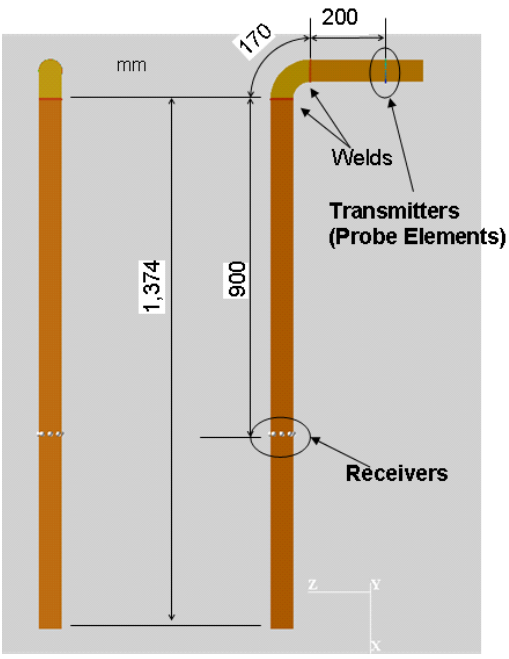

Outer diameter = 60mm
Thickness = 4 mm

(a) Overview of model

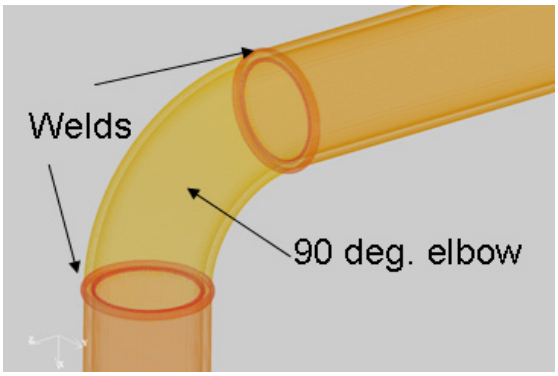

(b) Enlarged view of elbow and welds

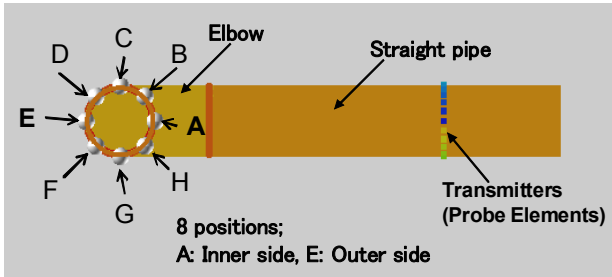

(c) Positions 8 receivers

Fig. 4. Two pipes and elbow model with two welds for prediction of T-mode guided wave propagation beyond elbow and welds (Model 3)

Table 1 Material parameters and simulation conditions

	Model 1	Model 2	Model 3
Material (Sound velocity and density)	Aluminum alloy base metal (Vl = 6.0 km/s, Vs = 3.04 km/s, density = 2.7 × 10^3 kg/m^3)	Type 304 stainless steel base metal (Vl = 5.7 km/s, Vs = 3.1 km/s, density = 7.9 × 10^3 kg/m^3)	Aluminum alloy base metal (Vl = 6.0 km/s, Vs = 3.04 km/s, density = 2.7 × 10^3 kg/m^3)
Dimensions	OD = 5 mm, t = 1 mm	OD = 34 mm, t = 3.2 mm	OD = 60 mm, t = 4 mm
Center frequency	200 kHz, 1,000 kHz	200 kHz	30 kHz, 50 kHz
Element size	0.1 mm × 0.1 mm × 0.1 mm	0.2 mm × 0.2 mm × 0.2 mm	0.5 mm × 0.5 mm × 0.5 mm

3. Results

3.1. Simulation results of Model 1 (L-mode guided wave propagation of different frequency)

Figure 5 shows the visualization results of the guided wave propagation in two pipes. The color bar indicates the magnitude of the absolute value of the displacement vector. The amplitude of the displacement vector of each wave packet in Fig. 5 is axisymmetric. Therefor, all wave packets propagate along the pipe axially symmetric. Figure 6 shows the group velocity dispersion curves of the L-mode propagating in a 5 mm outer diameter and 1 mm thickness aluminum pipe. The vertical black-dotted lines indicate the excitation frequencies, at 200 kHz and 1,000 kHz. Considering the dispersion curves in Fig. 6, a wave packet at 200 kHz seems to be the L(0,1) mode. A faster wave packet at 1,000 kHz seems to be the L(0,2) and a slower wave packet seems to be the L(0,1) mode. Figure 7 shows an axial section of the Model 1. Details of the displacement vector of each wave packet are shown in Fig. 7. The red-dotted lines indicate the deformation of outer and inner surface. The green arrows indicate the displacement vector. The deformation of the pipe by the wave packet at 200 kHz was axisymmetric (The snapshot showed the wave packet expanded the diameter of the pipe.). Because the outer and inner surfaces of the pipe deformed in the same direction, the deformation in the wall direction was asymmetric. Therefore, this wave packet was identified as the L(0,1) mode [9][10]. The slower wave packet at 1,000 kHz was also identified as the L(0,1) mode.

The deformation of the pipe by the faster wave packet at 1,000 kHz was axisymmetric. However, in this case, the outer and inner surfaces of the pipe deformed in opposite directions, and the deformation in the wall direction was symmetric. Therefore, this wave packet was identified as the L(0,2) mode [9][10]. The wave modes of all wave packets were identified. Good agreement between FEM results and theoretical prediction through dispersion curves was obtained.

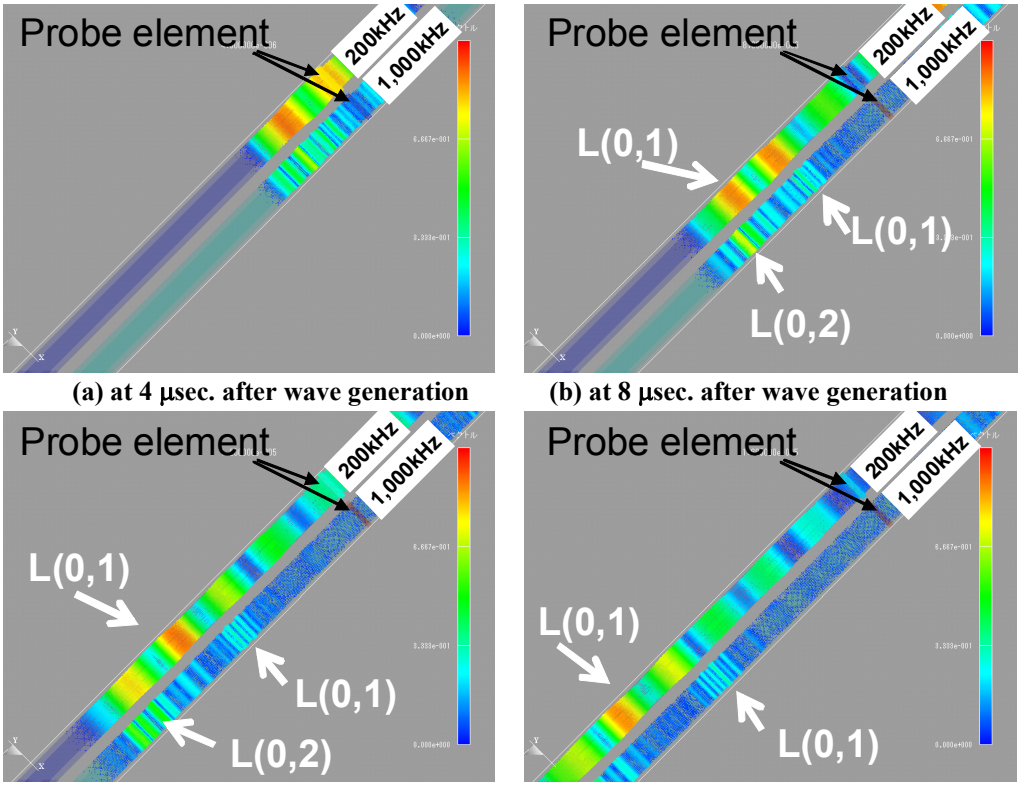

(a) at 4 μsec. after wave generation **(b) at 8 μsec. after wave generation**

(c) at 12 μsec. after wave generation **(d) at 16 μsec. after wave generation**

Fig. 5. Simulation results of L-mode guided wave propagation in Model 1 (200 kHz and 1,000 kHz)

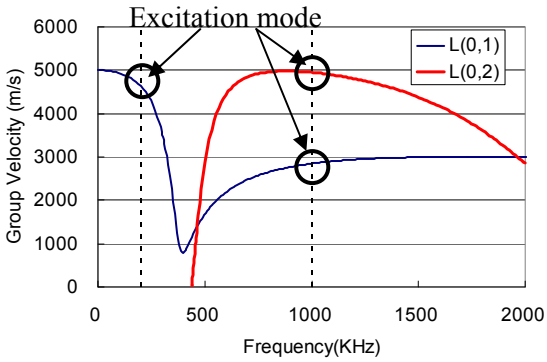

Fig. 6. Group velocity dispersion curves of L-modes propagating in a 5 mm outer diameter and 1 mm thickness aluminum alloy pipe

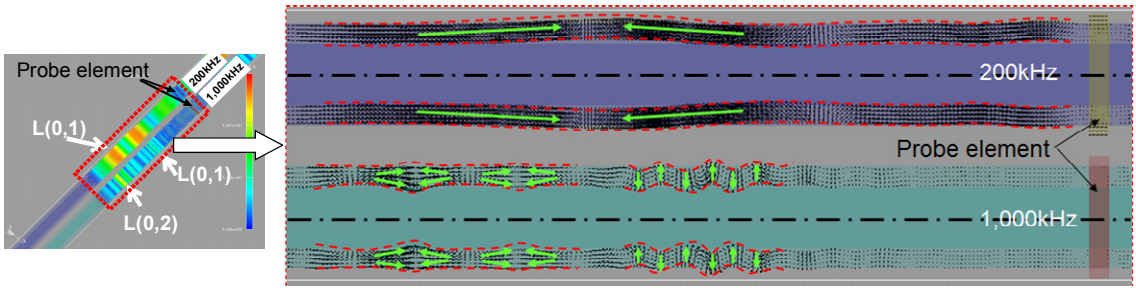

Fig. 7. Displacement vector of wave packets in Model 1 (axial section of the pipes)

3.2. Simulation results of Model 2 (Echo simulation from the pipe edge of L-mode guided wave)

Figure 8 shows simulation results, group velocity dispersion curves of the L-mode propagating in the pipe, and an experimental result of a received waveform [8]. Figure 8(a) shows the simulation result of a received waveform and Fig. 8(b) shows a visualization of the L-mode guided wave propagation that is indicated in the dispersion curves as shown in Fig. 8(c). The vertical red-dotted line indicates the excitation frequency. In this case, simulation results show that two types of the L-mode guided waves propagated toward the edges of the pipe, as shown in Fig. 8(b), and reflected at both the edges. Furthermore, echo signals were received as indicated in Fig. 8(a). The time of flight of the faster echo was around 400 μs and that of the slower echo was around 700 μs. Figure 8(d) shows an experimentally received waveform that was detected using a special optical fiber sensor [8].

Figures 8(a) and 8(d) show that the time of flight of each echo in the simulated and experimentally received waveform was almost equal. We have not modeled characteristics of the optical fiber sensor yet. Therefor, the simulation does not predict the amplitude of echoes completely. Comparisons between the FEM simulation and the experimental results show that the FEM simulation corresponds very well to the state (the two modes having different propagation times and amplitudes) of guided wave propagation in the actual piping.

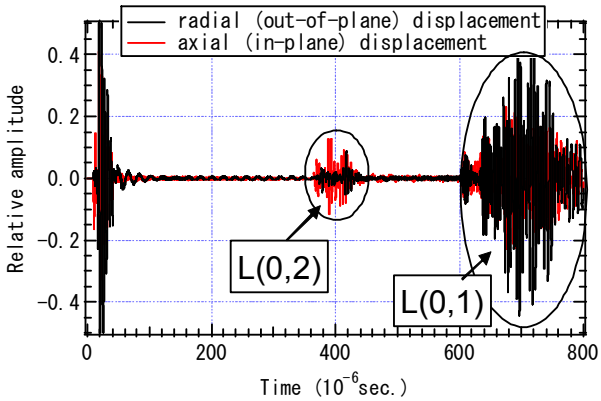

(a) Simulation result of received waveform

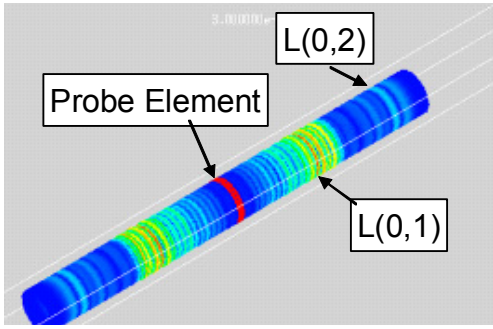

at 20 μsec.

(b) Visualization of L-mode guided wave propagation

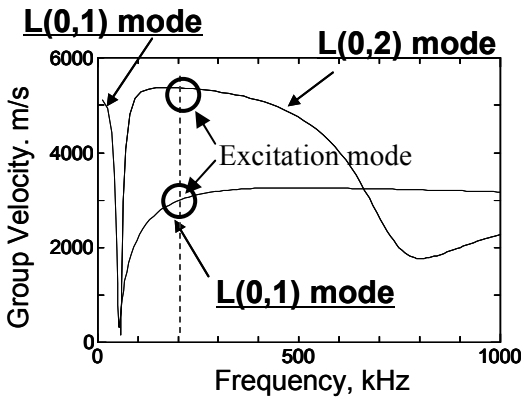

(c) Group velocity dispersion curves

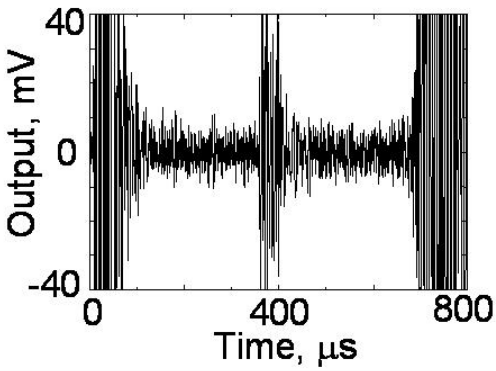

(d) Experimental received waveform

Fig. 8. Simulation results, group velocity dispersion curves of L-modes propagating in a 34 mm outer diameter and 3.2 mm thickness stainless steel pipe, and experimental received waveform[8]

3.3. Simulation results of Model 3 (T-mode guided wave propagation beyond welds and elbow piping)

Figures 9(a) and 9(b) show simulation results of received waveforms at eight different positions as shown in Fig. 4(c). These waveforms are circumferential components of the displacement vector. The signals at the top of the figures are sums of the eight signals, that are fundamental T(0,1) mode. In Fig. 9(a), the echo of the fundamental T(0,1) mode appears only around at 500 μs. Each waveform

also has large echo amplitude at a propagation time of around 500 μs. The echo durations of positions A, B, D, E, F, and H are longer than those of the fundamental T(0,1) mode. The delayed part of the echo may be a different mode from the T(0,1) mode. Sound velocity of the mode is slower than that of the T(0,1) mode. Because the phases of the waveforms at around 600 μs of positions A and E are opposite in direction, an asymmetric mode may be generated beyond the elbow.

In Fig. 9(b), large echo amplitude appears at 50 kHz at a propagation time of around 450 μs. A delayed echo clearly appears at a propagation time of around 600 μs in positions A, C, E, and G at 50kHz. The waveforms at around 600 μs of positions A and E have a coordinate phase. The phases of the waveforms at around 600 μs of positions A and C are opposite in direction. Therefore, asymmetric modes may be generated beyond the elbow at 50 kHz. Figure 10 shows snapshots of the displacement vector, which are cross-sectional views of the receiver position; at propagation times of around 450 and 600 μs. Figure 10(a) shows symmetrical and circumferential displacement vectors at 450 μs. Circumferential displacement vectors are shown in Fig. 10(b) corresponding to the receiver positions A, C, E, and G at 603 μs. This mode seems to be a higher order of T-mode [11].

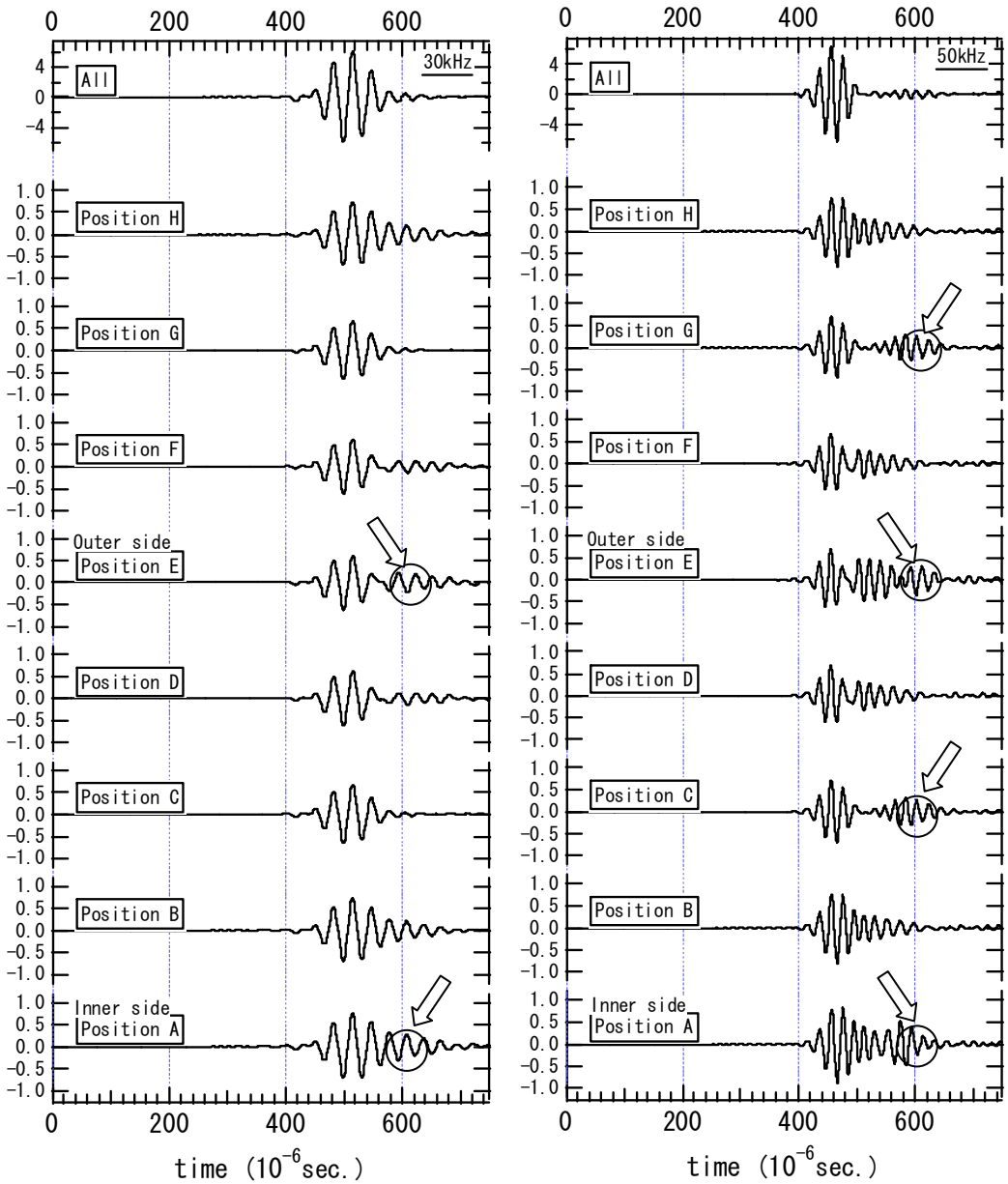

(a) at 30 kHz T-mode **(b) at 50 kHz T-mode**

Fig. 9. Waveforms received at eight positions and addition of eight waveforms beyond elbow and welds

To investigate the cause of these phenomena, the visualization results of guided wave propagation in elbow and beyond are displayed in Figs. 11 and 12. The color bar corresponds to the amplitude of the absolute value of the displacement. Symmetric wave packets are seen in Figs. 11(a) and 12(a). The simulation results indicated the mode-conversion to asymmetric modes beyond the elbow. The FEM results show that the difference between the traveling paths of the inner and outer sides of the elbow is one of the major causes of the asymmetric modes.

When the 30 kHz T-mode guided wave propagated in the elbow, the amplitude of the inner side was larger than that of the outer side as shown in Figs. 11(b) and (c) by natural focusing. In contrast, natural focusing to the outer side of the elbow is shown in Figs. 12(b) and (c) at 50 kHz. The visualization results of guided wave propagation revealed that the natural focusing position was changed depending on the excitation frequency.

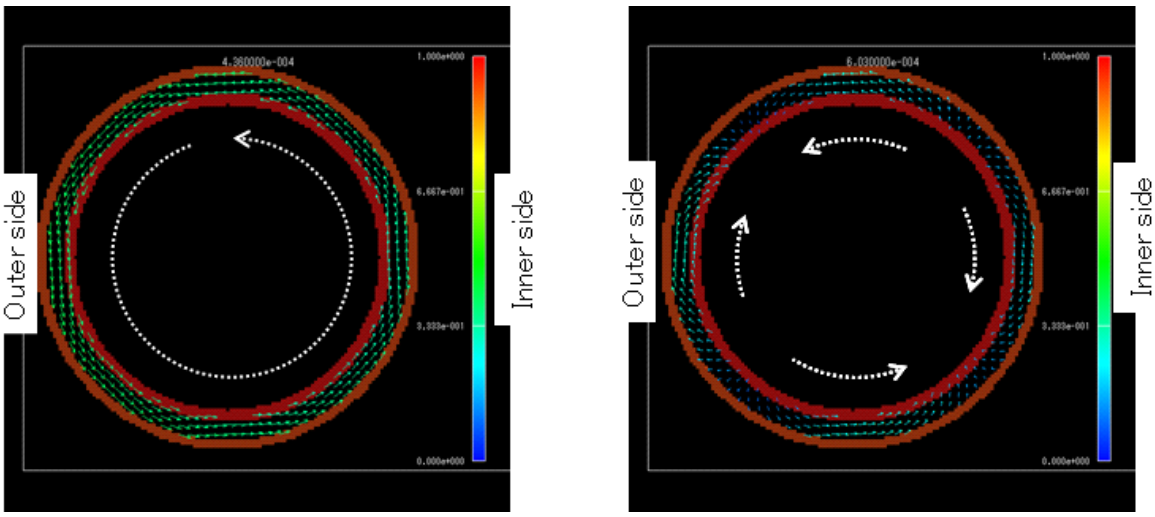

(a) at 450 μsec. **(b) at 603 μsec.**

Fig. 10. Cross sectional snap shots of displacement vector at received position (50 kHz)

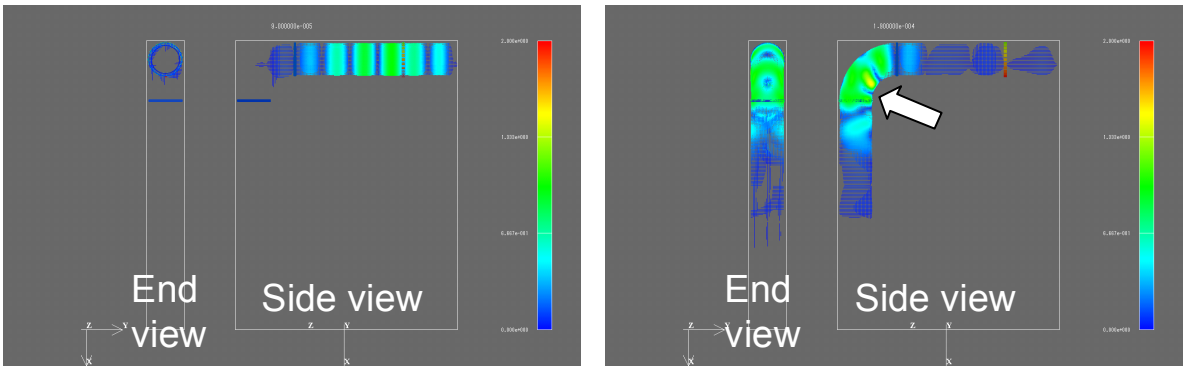

(a) at 90 μsec. after wave generation **(b) at 190 μsec. after wave generation**

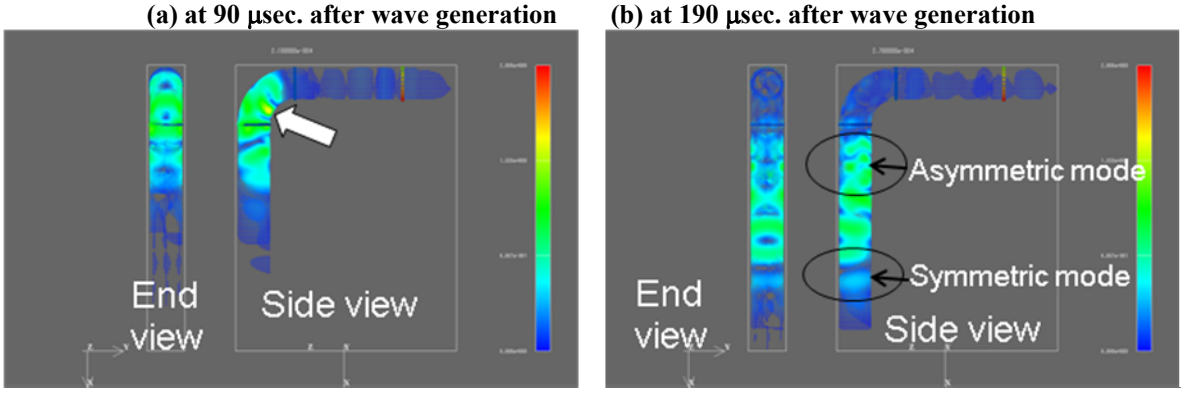

(c) at 210 μsec. after wave generation **(d) at 270 μsec. after wave generation**

Fig. 11. Visualized guided waves in elbow and beyond elbow region, at 30 kHz T-mode generation (The white arrows indicate the guided wave focusing due to the elbow.)

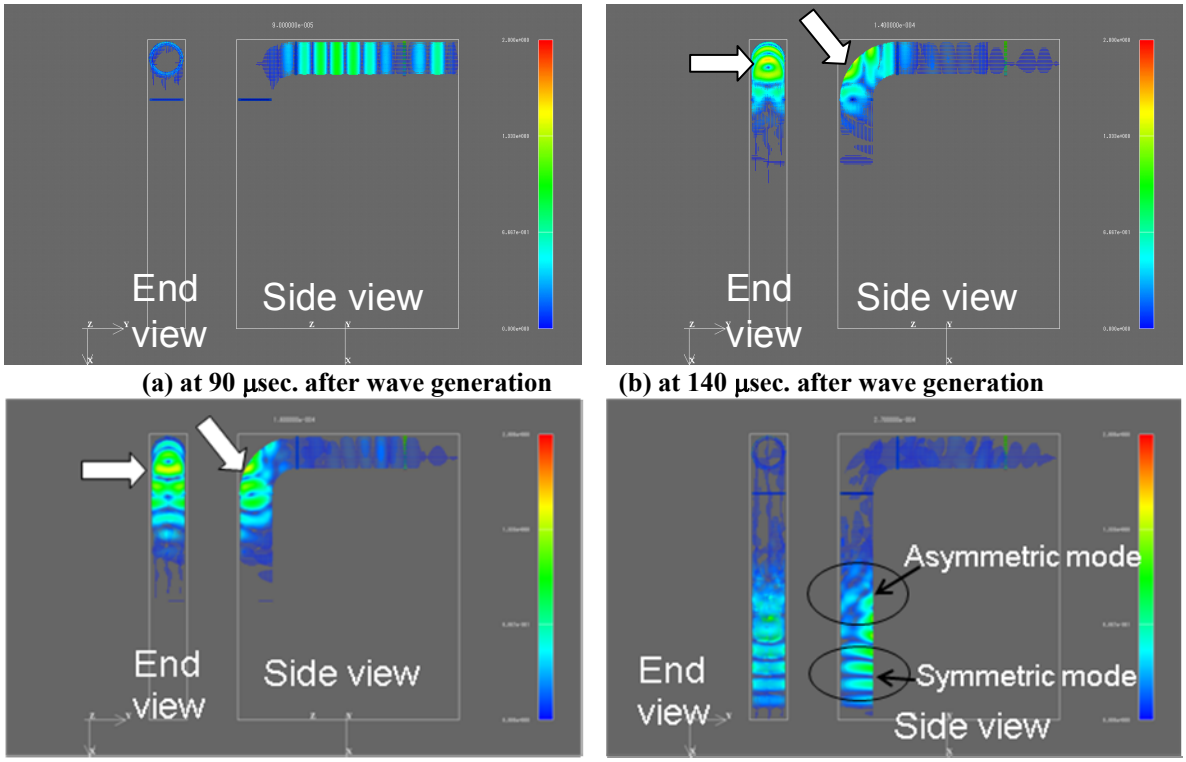

(a) at 90 μsec. after wave generation **(b) at 140 μsec. after wave generation**

(c) at 160 μsec. after wave generation **(d) at 270 μsec. after wave generation**

Fig. 12. Visualized guided waves in elbow and beyond elbow region, at 50 kHz T-mode generation (The white arrows indicate the guided wave focusing due to the elbow.)

4. Conclusion

3D large-scale FEM models were employed to simulate guided wave propagation in straight pipes and pipes with elbows. The accuracy of this FEM model was verified. The simulation results showed that the higher-order of T-modes were generated beyond the elbow by mode-conversion. The natural focusing occurred in the elbow. The focal positions of 30 kHz and 50 kHz T-mode guided wave were the inner side and the outer side, respectively. The simulation results also showed that the frequency dependence of the natural focal position of the T-mode guided wave in the elbow.

Acknowledgement

We would like to thank Dr. H. Nishino of Tokushima University for the valuable discussions during this investigation.

References

[1] Joseph L. Rose, "Ultrasonic Guided Waves: An Introduction to the Technical Focus Issue", Materials Evaluation, Vol. 61, 2003, p.65

[2] C H P Wassink, M A Robers, J A de Raad and T Bouma, "Condition monitoring of inaccessible piping", Insight, Vol. 43, pp.86-88

[3] P. Cawley, M.J.S. Lowe, D.N. Alleyne, B. Pavlakovic and P. Wilcox, "Practical Long Range Guided Wave Testing: Applications to Pipes and Rail", Materials Evaluation, Vol. 61, 2003, pp.66-74

[4] Hegeon Kwun, Sang Y. Kim and Glenn M. Light, "The Magnetostrictive Sensor Technology for Long Range Guided Wave Testing and Monitoring Structures", Materials Evaluation, Vol. 61, 2003, pp.80-84

[5] Joseph L. ROSE, Jing MU, Younho CHO, "Recent Advances on Guided Waves in Pipe

Inspection", 17th WCNDT, 25-28 Oct. 2008
[6] Takahiro Hayashi and Joseph L. Rose, "Guided Wave Simulation and Visualization by a Semianalytical Finite Element Method", Materials Evaluation, Vol. 61, 2003, pp.75-79
[7] http://www.ctc-g.co.jp/
[8] T. Matsuo, H. Cho and M. Takemoto, "Evaluation of Corrosion-induced Wall Reduction of Pipe using both Optical Fiber AE System and Guided Wave Inspection Method", Zairyo Shiken Gijutu, Vol.52, 2007, pp.154-161 (in Japanese)
[9] Joseph L. ROSE, " Ultrasonic waves in solid media", Cambridge Univ. press, 1999, pp.159-161
[10] H. Nishino, S. Takahashi, F. Uchida, M. Takemoto and K. Ono, "Modal Analysis of Hollow Cylindrical Guided Wave and Applications", Jpn. J. Appl. Phys. Vol.40, 2001, pp.364-370
[11] H. Nishino, T. Tanaka, S. Katashima and K. Yoshida, "An experimental investigation of mode conversions of the T(0,1) mode guided wave propagating in an elbow pipe", Jpn. J. Appl. Phys. Vol.50, 2011, 046601